

## Mechanical optic neuropathy in high myopia

*Clin Exp Optom* 2017

DOI:10.1111/cxo.12548

**Georgios Bontzos**\*<sup>†</sup> MD MSc  
**Sotiris Plainis**\*<sup>†‡</sup> MSc PhD  
**Efrosini Papadaki**<sup>§</sup> MD PhD  
**Trisevgeni Giannakopoulou**\*<sup>†</sup> MSc  
**Efstathios Detorakis**\*<sup>†</sup> MD PhD

\*Department of Ophthalmology, University Hospital of Heraklion, Heraklion, Greece

<sup>†</sup>Institute of Vision and Optics, University of Crete, Heraklion, Greece

<sup>‡</sup>Faculty of Life Sciences, University of Manchester, Manchester, UK

<sup>§</sup>Department of Radiology, University Hospital of Heraklion, Heraklion, Greece

E-mail: gbontzos@hotmail.gr

Submitted: 17 December 2016

Revised: 21 February 2017

Accepted for publication: 25 February 2017

**Key words:** acceleration, mechanical damage, optic nerve, pathologic myopia

Myopia is a major cause of visual impairment and its prevalence is increasing globally at an alarming rate. High pathologic myopia is described as myopia with associated degenerative changes in the sclera, choroid and retinal pigment epithelium, resulting initially in loss of visual acuity (VA).<sup>1</sup> Excessive elongation of the globe and posterior staphyloma are the hallmark findings in pathological myopia leading to mechanical damage to the retina and the optic nerve as a result of global stretching.<sup>2</sup> Lacquer cracks, representing mechanical breaks of Bruch's membrane are a typical manifestation of mechanical stretching in high myopic eyes.<sup>3</sup> Moreover, papillary and peripapillary regions are often distorted because of the mechanical stress caused by an elongated myopic eye causing tilted optic discs<sup>4</sup> and acquired megalodiscs.<sup>5</sup>

This report describes a case of a 43-year-old Caucasian man with pathological myopia who reported decreased vision in his right eye after an airplane landing. Imaging and clinical workup revealed excessive

globe elongation potentially leading to optic nerve dysfunction.

### CASE REPORT

A 43-year-old highly myopic male patient was referred to the Department of Ophthalmology of the University Hospital in Heraklion, Greece, with blurry vision and partial impairment in the nasal visual field of his right eye. Symptoms appeared immediately after landing from a long flight journey. He complained of perceiving a distorted image with the effect being more pronounced in his right eye. His past medical history was unremarkable. He was not on any medication, was not drinking any alcohol or smoking tobacco. His ophthalmic history was significant for high myopia resulting in retinal breaks treated with green-laser in both eyes 20 years ago and LASIK refractive surgery, 14 years before the incident (preoperative spherocylindrical error was  $-9.00/-1.50 \times 15^\circ$  [RE]  $-8.00/-1.25 \times 180^\circ$  [LE]). Myopia did progress in both eyes post-operatively associated with further axial elongation, resulting in a current spherocylindrical error of  $-9.00/-1.50 \times 75^\circ$  (RE) and  $-7.75/-1.50 \times 100^\circ$  (LE), by the time he was referred. Axial length (IOL Master, Carl Zeiss, Jena, Germany) was found to be 33.7 mm and 34.6 mm R and L, respectively.

On ophthalmological examination, VA was found to be 6/9.6 R and 6/7.5 L. Slitlamp biomicroscopic findings were compatible with previous LASIK surgery in both eyes, while funduscopy was significant for a highly myopic fundus with parapapillary atrophic gamma zone with no signs of disc swelling. Optical coherence tomography and fundus fluorescein angiography were non-contributory. Automated perimetry (Medmont, Melbourne, Victoria, Australia) was significant for enlarged blind spots in both eyes, compatible with changes related to the pathological myopia; however, in the right eye a centro-caecal

scotoma extending to the temporal borders of the macular area was also evident (Figure 1).

Magnetic resonance imaging revealed ocular elongation in anterior–posterior direction and a posterior protrusion along the visual axis. Interestingly, the intraorbital optic nerve pathway was grossly distorted as shown in the T2 fat-saturation sagittal image of the orbital apex, forming a steep curve from the posterior pole of the eyeball to the posterior-nasal apex of the globe in both eyes but more pronounced on the right side where a sharp kink in the course of the optic nerve may render it sensitive to mechanical stress (Figure 2).

In an attempt to obtain objective information regarding the visual function of the patient's International Society for Clinical Electrophysiology of Vision standard,<sup>6,7</sup> visual electrodiagnosis was performed. Full-field light-evoked electroretinograms (ERG) were recorded using the Primus 2.5 system (Tomey, Nürnberg, Germany) and corneal silver-nylon thread DTL electrodes. Both cone- and rod-specific responses were found reduced compared to lower limits of normal levels (Figure 3) but since a linear reduction in ERG amplitude with increasing axial length has been observed,<sup>8</sup> expected amplitudes were derived and found to be within normal limits.

Visual evoked potentials (VEP) were elicited using reversing 30 and 15 arcmin checks of 100 per cent contrast at a rate of four reversals per second (two Hertz) with square-wave temporal modulation (space-averaged luminance was  $30 \text{ cd/m}^2$ ). The waveforms were amplified (gain = 10 K) using the CED 1902 (Cambridge Electronic Design, Cambridge, UK). Data acquisition and averaging were controlled using the Signal software (vs. 3.1, Cambridge Electronic Design). Each VEP trace was the average of 64 epochs of one-second duration each. P100 peak amplitude and latency were derived from the average waveform. P100 amplitude was found

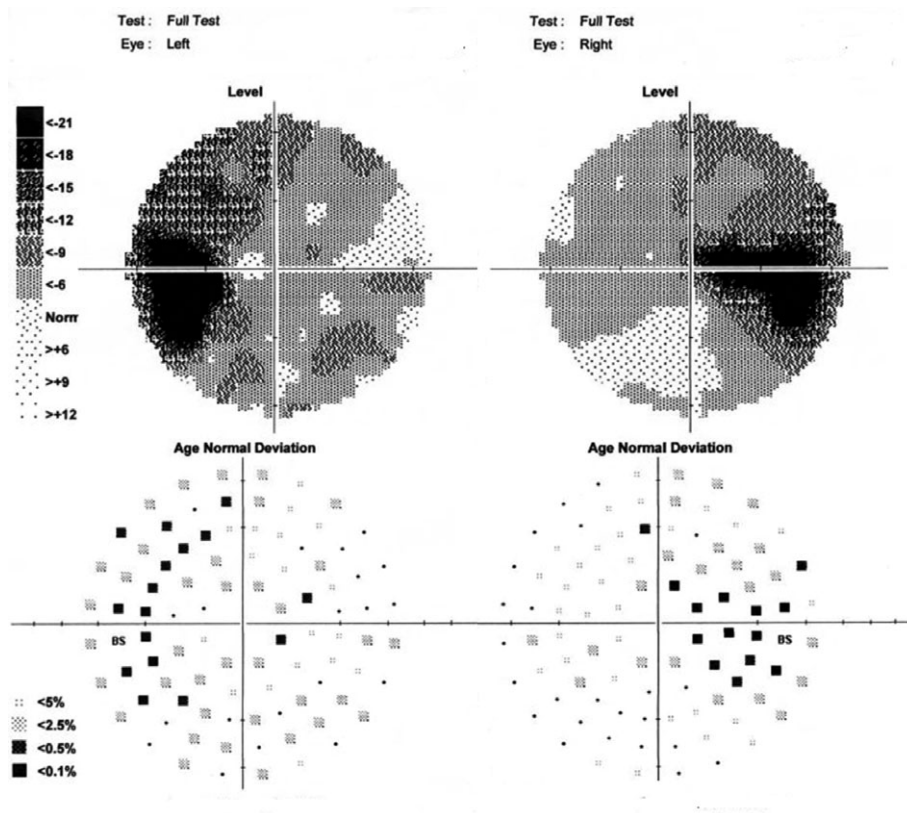


Figure 1. Visual fields showing central visual defect in the peripapillary distribution and inferior nasal depression in the right eye

decreased in both eyes for both check sizes compared to normal responses (Figure 3) but more pronounced was the characteristic delaying P100 latency (of about 49 and 52 ms in both eyes compared to average values of volunteers with normal vision<sup>9</sup> [average age  $28 \pm 5$  years] for 30 and 15 arcmin check size, respectively).

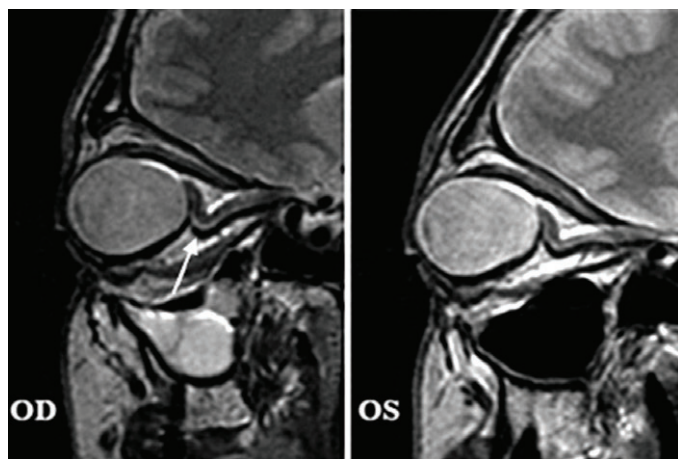


Figure 2. Optic nerve pathway is distorted, as shown in the T2 fat-saturation sagittal image of the orbital apex and forms a curve in its intraorbital segment. The retrobulbar kink of the optic nerve course, more pronounced in the right side, is shown with a white arrow.

## DISCUSSION

Given the lack of other systemic findings and negative medical workup, his symptoms could be attributed to gravitational or acceleration-deceleration forces generated by the airplane landing. Such forces could create mechanical stretch to an already distorted and elongated optic nerve and eyeball. A transient reduction of VA under acceleration has been reported previously and associated with changes in aqueous humour flow;<sup>10,11</sup> however, in this case, the symptoms remained stable over his follow-up examinations for about a year.

The gravitational force (G-force) on a body is its acceleration relative to the free-fall. The term is used as a value for measuring acceleration. Although tissues and organs can withstand high positive and negative values of G-force (during acceleration and deceleration, respectively), rapid changes may be associated with ocular injuries.<sup>10,12</sup> Retinal and sub-conjunctival haemorrhages are the most common ocular complications. The proposed mechanism is that a rapid acceleration would increase the intravenous pressure. At emergent acceleration, blood would accumulate in the lower limbs, leading to ischaemia and hypoxia of the brain and eyes, resulting in visual impairment, such as transient visual loss of central or peripheral vision and loss of consciousness after encountering a high acceleration.<sup>13</sup>

Yet, another suggested mechanism refers to changes in intra-thoracic, intra-abdominal and intracranial hydrostatic pressure, the latter transmitted through the optic nerve.<sup>14,15</sup> In this patient, due to the myopic morphological changes, the lamina cribrosa is expected to be stretched and thinned,<sup>16</sup> reducing the distance between the two compartments. This steepens the pressure gradient, making the patient's already deformed optic nerve even more susceptible to damage after shifts in intracranial pressure. Moreover, by increasing in the aperture of the peripapillary sclera flange opening but with the optic nerve remaining constant in size, the peripheral posterior surface of the lamina cribrosa is no longer covered and buffered by the solid tissue of the optic nerve head but gets exposed to the orbital cerebrospinal fluid.<sup>17</sup> As the fluid offers less mechanical resistance against deformation than the solid optic nerve tissue, pressure-related pathological changes may predominantly

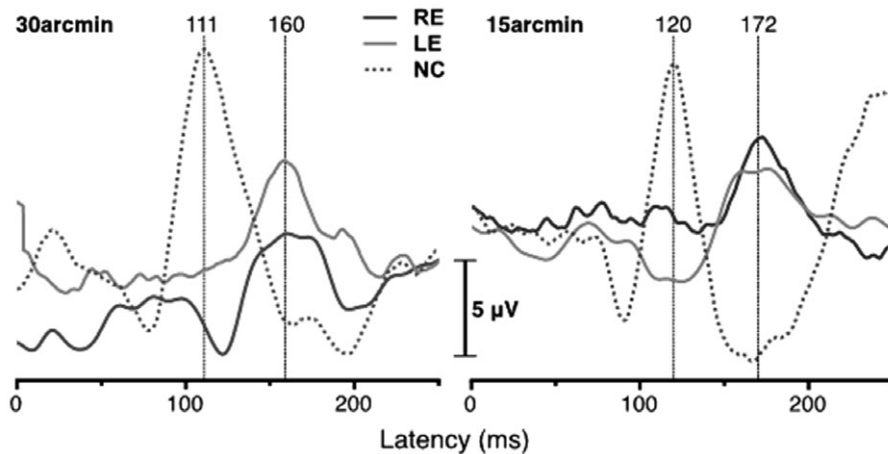


**Figure 3.** Grand-averaged (64 epochs) monocular visual evoked potential (VEP) waveforms elicited using two Hertz-reversing 30 (left) and 15 (right) arcmin checks of 100 per cent contrast for the right eye (black line) and left eye (grey line) of the patient and for volunteers with normal vision<sup>9</sup> (average age  $28 \pm 5$  years, dotted lines). P100 latency is indicated in milliseconds.

take place in the periphery of the lamina cribrosa close to the optic disc border.<sup>18</sup>

Human orbits contain enough orbital soft tissue (retrobulbar fat pads), tight fibrous compartments and ligaments allowing for an unobstructed but controlled, globe movement within the orbit. These tissues are subjected to mechanical loading from external forces on the eye. Optic nerves are firmly attached to the sclera and to the orbital apex, so violent translational movements of the globe could generate severe tractional forces at these sites. The patient's orbit in this case has less space-protective soft tissue as a result of his elongated eyeball. Expansion of the posterior portion of myopic eyes may alter the anatomic relationships in and around the optic nerve, leading to connective tissue remodelling.<sup>19</sup> Disorders such as heavy eye syndrome have been reported and associated with pathological myopia on the basis of the idea that the longer, more myopic eye is in a relatively low position, as though it was too heavy. The causation appears to be an abnormally low muscle path of the lateral rectus in the involved eye, provoking hypophoria or hypotropia.<sup>20</sup> The relative volume of osseous and soft tissue orbital structures may affect the protrusion of orbital contents and the vital space for the intraorbital optic segment. This concept is described as effective orbital volume (that

is, the difference between orbital and eyeball volume).<sup>21,22</sup>

The patient presented in this case developed a visual field scotoma in his right eye, which, based on perimetry, imaging and ERG findings may be associated with optic nerve dysfunction. A partial explanation for this could be axonal death following optic nerve compression under acceleration, which is also supported by his VEP recordings. The VEP P100 latency is substantially increased, much higher than the delays usually observed in optic neuritis<sup>23,24</sup> or in cases of reduced pupil apertures and/or decreased retinal luminance.<sup>26</sup>

#### REFERENCES

- Morgan IG, Ohno-Matsui K, Saw SM. Myopia. *Lancet* 2012; 379: 1739–1748.
- Wang S, Wang Y, Gao X et al. Choroidal thickness and high myopia: a cross-sectional study and meta-analysis. *BMC Ophthalmol* 2015; 15: 70.
- Neelam K, Cheung CM, Ohno-Matsui K et al. Choroidal neovascularization in pathological myopia. *Prog Retin Eye Res* 2012; 31: 495–525.
- You QS, Xu L, Jonas JB. Tilted optic discs: The Beijing Eye Study. *Eye (Lond)* 2008; 22: 728–729.
- Jonas JB. Optic disk size correlated with refractive error. *Am J Ophthalmol* 2005; 139: 346–348.
- Marmor MF, Fulton AB, Holder GE et al. ISCEV Standard for full-field clinical electroretinography (2008 update). *Doc Ophthalmol* 2009; 118: 69–77.
- Odom JV, Bach M, Brigell M et al. ISCEV standard for clinical visual evoked potentials: (2016 update). *Doc Ophthalmol* 2016; 133: 1–9.

- Westall CA, Dhaliwal HS, Pantou CM et al. Values of electroretinogram responses according to axial length. *Doc Ophthalmol* 2001; 102: 115–130.
- Plainis S, Petratou D, Giannakopoulou T et al. Binocular summation improves performance to defocus-induced blur. *Invest Ophthalmol Vis Sci* 2011; 52: 2784–2789.
- Byrnes VA. Elevated intravascular pressure as an etiologic mechanism in the production of eye injuries. *Trans Am Ophthalmol Soc* 1959; 57: 473–538.
- Tsai ML, Liu CC, Wu YC et al. Ocular responses and visual performance after high-acceleration force exposure. *Invest Ophthalmol Vis Sci* 2009; 50: 4836–4839.
- Curtis EB, Collin HB. Ocular injury due to bungee jumping. *Clin Exp Optom* 1999; 82: 193–195.
- Fitt AD, Gonzalez G. Fluid mechanics of the human eye: aqueous humour flow in the anterior chamber. *Bull Math Biol* 2006; 68: 53–71.
- Whinnery JE, Whinnery AM. Acceleration-induced loss of consciousness. A review of 500 episodes. *Arch Neurol* 1990; 47: 764–776.
- Smith DC, Kearns TP, Sayre GP. Preretinal and optic nerve-sheath hemorrhage: pathologic and experimental aspects in subarachnoid hemorrhage. *Trans Am Acad Ophthalmol Otolaryngol* 1957; 61: 201–211.
- Jonas JB, Berenshtein E, Holbach L. Anatomic relationship between lamina cribrosa, intraocular space and cerebrospinal fluid space. *Invest Ophthalmol Vis Sci* 2003; 44: 5189–5195.
- Jonas JB, Xu L. Histological changes of high axial myopia. *Eye (Lond)* 2014; 28: 113–117.
- Campbell IC, Coudrillier B, Ross Ethier C. Biomechanics of the posterior eye: a critical role in health and disease. *J Biomech Eng* 2014; 136: 021005.
- Rutar T, Demer JL. 'Heavy Eye' syndrome in the absence of high myopia: A connective tissue degeneration in elderly strabismic patients. *J AAPOS* 2009; 13: 36–44.
- Tan RJ, Demer JL. Heavy eye syndrome versus sagging eye syndrome in high myopia. *J AAPOS* 2015; 19: 500–506.
- Detorakis ET, Drakonaki EE, Papadaki E et al. Evaluation of globe position within the orbit: clinical and imaging correlations. *Br J Ophthalmol* 2010; 94: 135–136.
- Detorakis ET, Maris T, Papadaki E et al. Evaluation of the position and function of aqueous drainage implants with magnetic resonance imaging. *J Glaucoma* 2009; 18: 453–459.
- Ringelstein M, Kleiter I, Ayzenberg I et al. Visual evoked potentials in neuromyelitis optica and its spectrum disorders. *Mult Scler* 2014; 20: 617–620.
- Kiiski HS, Ni Riada S, Lalor EC et al. Delayed P100-like latencies in multiple sclerosis: a preliminary investigation using visual evoked spread spectrum analysis. *PLoS One* 2016; 11: e0146084.
- Plainis S, Petratou D, Giannakopoulou T et al. Interocular differences in visual latency induced by reduced-aperture monovision. *Ophthalmic Physiol Opt* 2013; 33: 123–129.
- Plainis S, Petratou D, Giannakopoulou T et al. Small-aperture monovision and the Pulfrich experience: absence of neural adaptation effects. *PLoS One* 2013; 8: e75987.